



LAWRENCE
LIVERMORE
NATIONAL
LABORATORY

LSST Telescope Guider Loop Requirements Analysis, and predicted Performance

M. Warner, J. Sebag, V. Riot

June 16, 2010

LSST Telescope Guider Loop Requirements Analysis, and predicted Performance.

San Diego, CA, United States

June 27, 2010 through July 2, 2010

Disclaimer

This document was prepared as an account of work sponsored by an agency of the United States government. Neither the United States government nor Lawrence Livermore National Security, LLC, nor any of their employees makes any warranty, expressed or implied, or assumes any legal liability or responsibility for the accuracy, completeness, or usefulness of any information, apparatus, product, or process disclosed, or represents that its use would not infringe privately owned rights. Reference herein to any specific commercial product, process, or service by trade name, trademark, manufacturer, or otherwise does not necessarily constitute or imply its endorsement, recommendation, or favoring by the United States government or Lawrence Livermore National Security, LLC. The views and opinions of authors expressed herein do not necessarily state or reflect those of the United States government or Lawrence Livermore National Security, LLC, and shall not be used for advertising or product endorsement purposes.

LSST Telescope Guider Loop Requirements Analysis, and predicted Performance.

Michael Warner^{*a}, Vincent Riot^b, Jacques Sebag^c

^aCerro Tololo Inter-American Observatory, Casilla 603, La Serena, Chile.

^bLawrence Livermore National Laboratory, 7000 East Ave., Livermore, CA, USA 94550

^cNational Optical Astronomy Observatory, 950 N. Cherry Ave., Tucson, AZ, 85719.

ABSTRACT

The LSST Telescope has critical requirements on tracking error to meet image quality specifications, and will require closing a guiding loop, with the telescope servo control, to meet its mission. The guider subsystem consists of eight guiding sensors located inside the science focal plane at the edge of the 3.5deg field of view. All eight sensors will be read simultaneously at a high rate, and a centroid average will be fed to the telescope and rotator servo controls, for tracking error correction. A detailed model was developed to estimate the sensors centroid noise and the resulting telescope tracking error for a given frame rate and telescope servo control system.

The centroid noise depends on the photo-electron flux, seeing conditions, and guide sensor specifications. The model for the photo-electron flux takes into consideration the guide star availability at different galactic latitudes, the atmospheric extinction, the optical losses at different filter bands, the detector quantum efficiency, the integration time and the number of stars sampled. A 7-layer atmospheric model was also developed to estimate the atmospheric decorrelation between the different guide sensors due to the 3.5deg field of view, to predict both correlated and decorrelated atmospheric tip/tilt components, and to determine the trade-offs of the guider servo loop.

Keywords: LSST, Guider Camera, Guiding Servo Loop, Atmospheric Tip-Tilt Model.

1. INTRODUCTION

The LSST Telescope has critical requirements on tracking error to meet the science image quality specifications. This requires closing a Guider loop and correcting the telescope pointing as needed to meet its mission. The Guider camera subsystem consists of eight guiding sensors located at the edge of the 3.5deg science field of view, as shown in Figure 1. The eight Guide sensors will be read simultaneously. Each guider star centroid will be calculated and the correction signals will be propagated to the Telescope Mount for pointing and camera rotator correction, closing a servo loop.

A model to test the critical centroid noise requirements was developed. This model incorporates all the internal and external variables that can affect centroid noise, which is then tested against a worst case scenario, where all conditions are taken to their limit, using the extreme environmental conditions from the LSST Operational Cadence Simulator (section 2.2). A guider/mount servo loop model was developed and includes the impact of the atmospheric decorrelation on tracking jitter. This is discussed in Section 3.

*mwarner@ctio.noao.edu; Phone: (56)-51-205-295

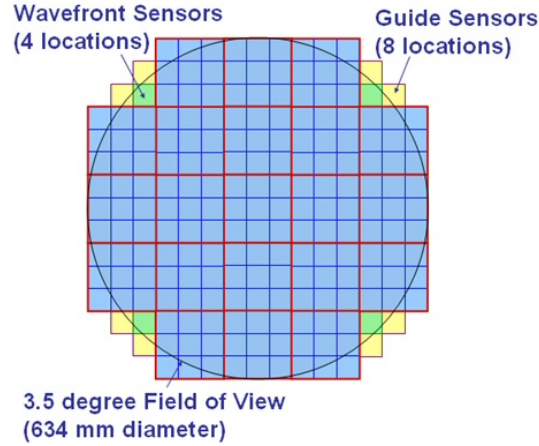


Figure 1. LSST Focal plane, showing the location of the 8 Guide Sensors.

2. OVERVIEW

2.1 LSST Guider Loop Requirements Model

A Guider Loop Requirements Model was constructed to analyze the trade-off between the different parameters that can affect the system performance. A block diagram of the model is shown in Figure 2. The critical parameters needed by the Telescope Subsystem: centroid noise, centroid frame rate, and transport delays, are analyzed in more detail in Section 3.1.

Some of the key requirements used for the analysis in this paper are shown in Table 1.

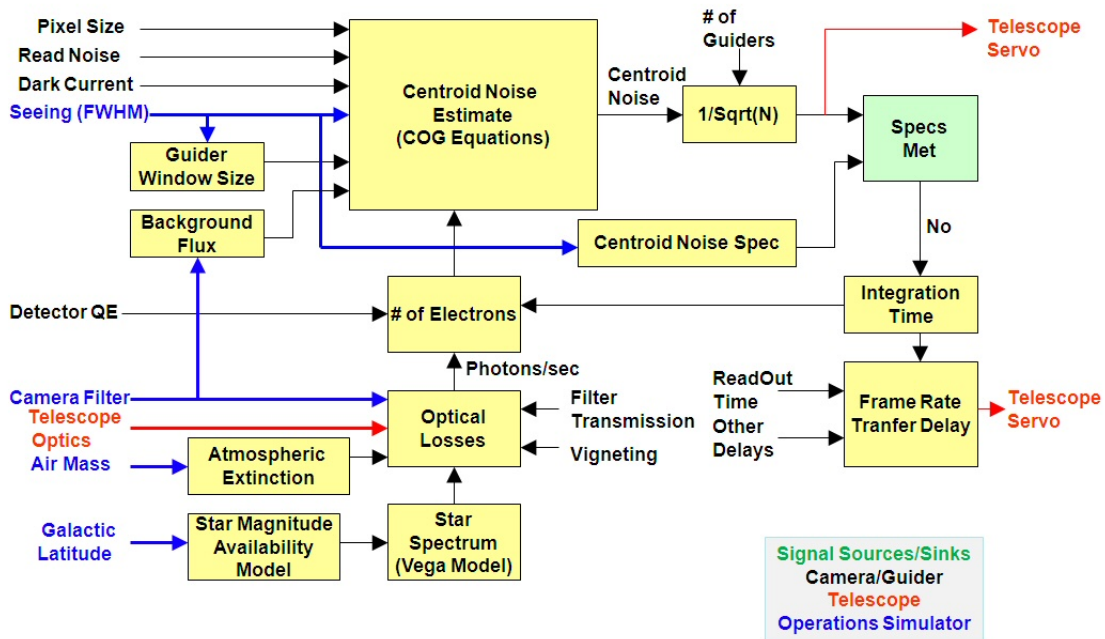


Figure 2. LSST Guider Loop Requirements Model.

Table 1. Guider Loop Key Requirements

Key Requirement	Value
Pixel Size	0.36 arcsec/pixel
Read-out Noise	18e- rms
Integration Time	100 ms
Total Transport Delays	10 ms
Frame Rate	9 Hz
Number of Guiders	8
Servo Loop Jitter for FWHM ≤ 0.6 arc-sec	0.02 arc-sec FWHM
Servo Loop Jitter for FWHM > 0.6 arc-sec	FWHM/30 arc-sec FWHM

2.2 LSST Guider Camera Optical Transmission Model

The LSST Guider Camera throughput was calculated by considering all the optical transmission of the atmosphere, telescope optics, camera optics, filter band, and HyViSI H2RG CMOS detector at 140K^{1,2} as shown in (Figure 3).

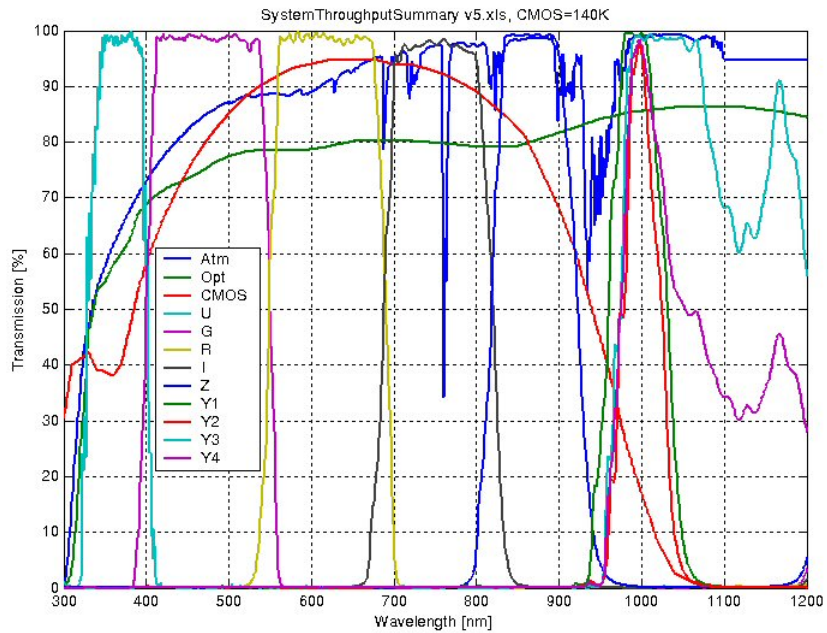


Figure 3. Baseline LSST Optical transmission (Air Mass=1.0)

Due to the location of the guider detector (Figure 1), the radial position of the guide sensors varies from 1.658, to 1.987 degrees from the center of the focal plane. Vignetting of the beam is present at these radial positions and is included in this analysis. The optical losses due to vignetting, and the guider detector surface area, as a function of the radial distance, are shown in Figure 4. The product of these two parameters yields an optimum trade-off point, at a radial distance of 1.9 degrees, where optical transmission due to vignetting is 64%, limiting the surface area used on the guider detector to 86%. These values were used in the analysis.

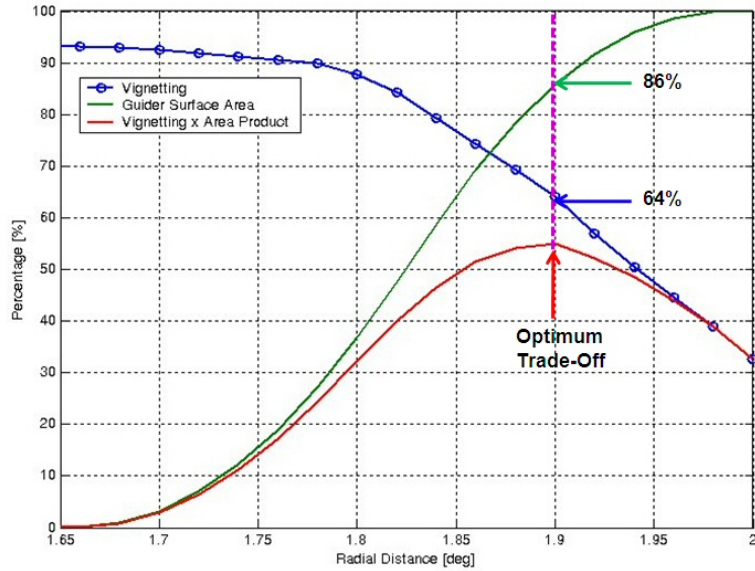


Figure 4. Guider Vignetting and Surface Area versus Radial Distance

Another important optical transmission parameter is Air Mass. In order to obtain a worst case value, the statistics obtained from the LSST Operational Cadence Simulator³ 10 year run were used, and the results are summarized in Figure 5. A worst case value of Air Mass=3.0 was used in the analysis.

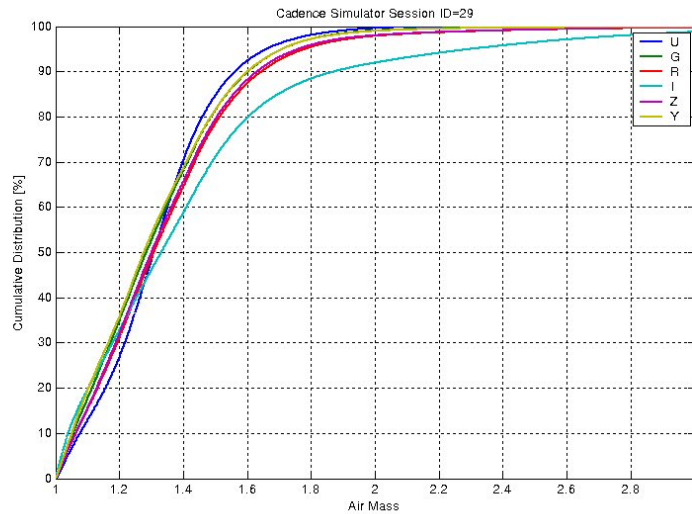


Figure 5. Air Mass Statistics from Cadence Simulator 10 year run.

In order to calculate the photon flux at the guider detector, a Vega Standard Spectral Model⁴ was obtained. The spectral Vega model was combined with the optical transmission from Figure 3. The resulting spectral flux at the guider, considering the LSST Telescope clear aperture, is shown in Figure 6.

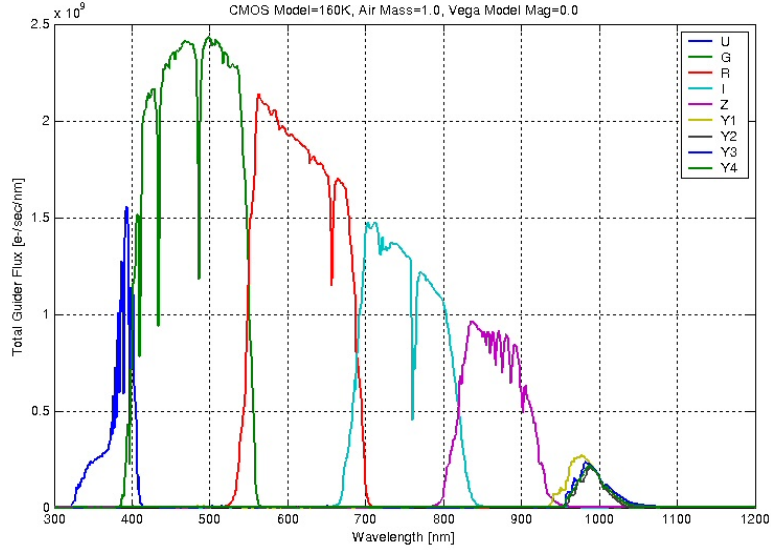


Figure 6. Guide Camera Spectral Flux for a Vega type spectra, Air Mass=1.0, at Magnitude=0.

2.3 LSST Guide Star Availability and Flux Statistics

The LSST Guide Star availability was adopted from C. W. Allen⁵, where the star population below a certain magnitude at different galactic longitudes is tabulated. A summary of this data is shown in Figure 7. This includes the smaller detector area of 86% as previously determined. The result shows that at a worst case condition of the galactic pole, a single 13.16 magnitude star should be found on each of the guider detector.

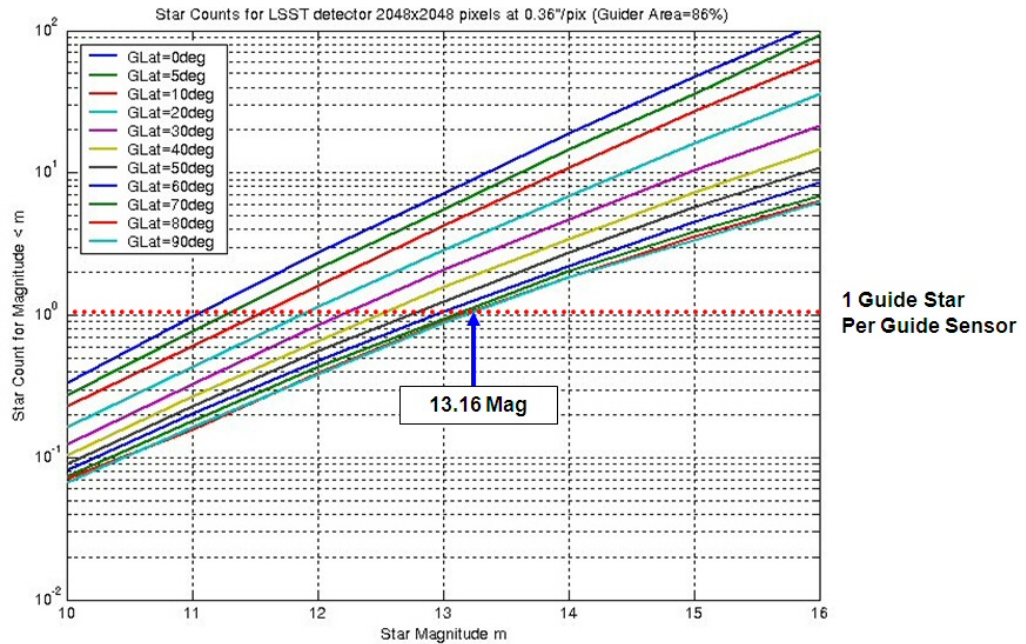


Figure 7. Star Count versus Magnitude at different galactic longitudes.

The spectral flux from Figure 6 was integrated for each filter band, and the total photo-electron flux was calculated for a 13.16 magnitude star, with an Air Mass=3.0, a vignetting of 64%, and a 100msec integration time. The resulting photo-electron count is shown in Figure 8. The lowest calculated flux in the Y2 filter band is equal to 2678 photo-electrons.

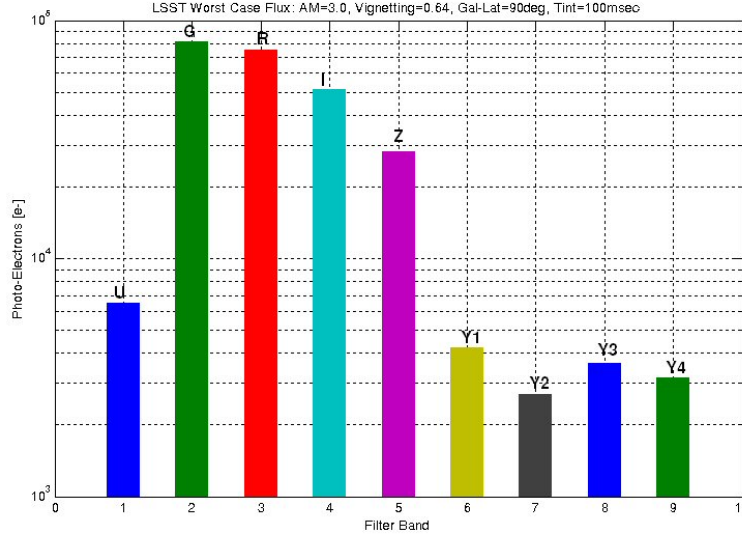


Figure 8. Worst case flux at different filter bands, for a 13.16 magnitude Vega type star.

2.4 LSST Guider Centroid Noise Analysis

The centroid noise depends on the photo-electron flux, seeing conditions, sky background flux, and guide sensor specifications such as pixel size, read and dark noise, as shown in Figure 2. The equation to calculate centroid noise (1) has been adapted from a centroid noise analysis used in Shack-Hartmann sensors⁶.

$$\sigma_c = pix \cdot \sqrt{\frac{(R_n^2 + B_{sky} + I_d)N_{pix}^4}{12N_{ph}^2} + \frac{N_T^2}{8\ln(2)N_{ph}}} \quad (1)$$

where pix is the pixel scale (arc-sec/pixel), R_n is the read noise (e-rms), B_{sky} is the sky background flux (e-), I_d is the dark noise during the integration time (e-), N_{pix}^2 is the total number of pixels in the guide window used for centroid computation, N_{ph} is the number of the photoelectrons from the guide star, and N_T is the seeing FWHM in pixels. The window size N_{pix} is modified as a function of seeing conditions to yield an optimum sampling of the guide star, of $2.55 \cdot FWHM$.

Using the nominal values from Table 1, and a sky background value of $3614.3e^-$ in 15sec (Y4-Band) from the sky background model developed for the science array⁷, a sky background value of $78.1e^-$ was found for the guider pixel size at 100 ms exposure time, and a dark noise value of $0.5e^-$ for the same exposure time. A worst case Guider/Mount Servo loop jitter due to centroid noise was calculated and the results are shown in Figure 9, including a value for the Servo Gain of 0.5, which is explained later in section 3.1.

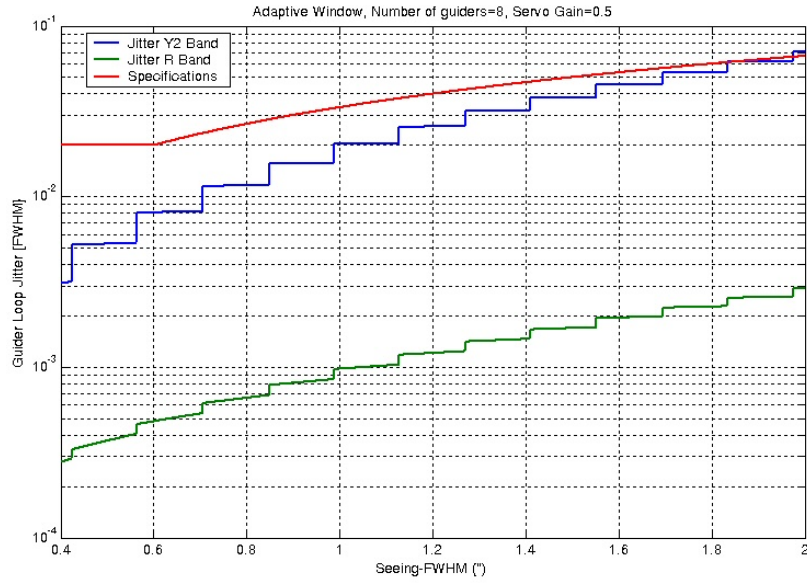


Figure 9. Guider Loop Jitter for different Seeing Conditions, for Y2 (2678e-) and R (75,336e-) Filter Bands

The Guider Loop worst case jitter, versus seeing can be compared against the seeing condition statistics obtained from the Cadence Simulator 10 yr run, and is shown in Figure 10. This shows that the Guider Loop jitter requirements can be met under all seeing conditions.

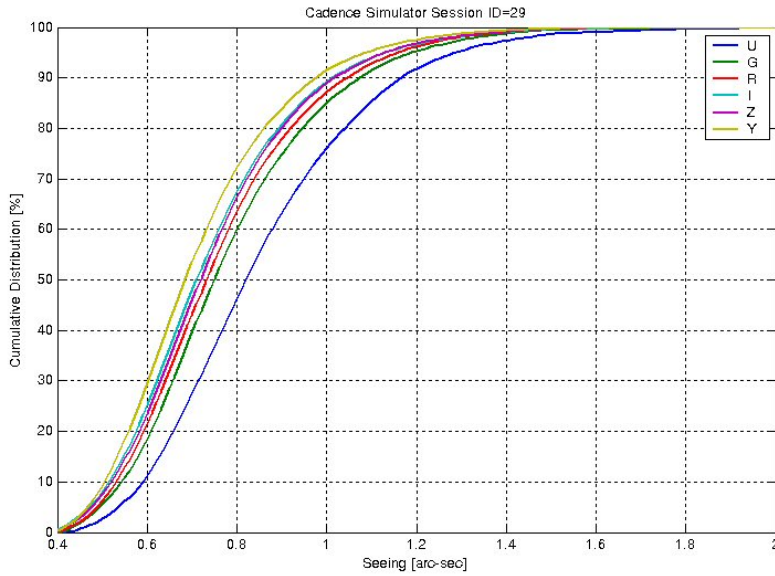


Figure 10. LSST seeing conditions cumulative distribution – Cadence Simulator 10yr run

3. GUIDER SERVO LOOP AND ATMOSPHERIC DECORRELATION

3.1 LSST Guider/Mount Servo Loop Description

A simplified model of the LSST Guider/Mount Servo loop is shown in Figure 11. The guider model consists of two components, the Total Delays, and a Zero Order Hold (ZOH) at the frame rate. Both of these components contribute delays which will destabilize a control system. The transport delay time component is shown in equation (2).

$$T_{\text{delay}} = T_{\text{int}}/2 + T_d \quad \text{Where: } T_{\text{int}} = \text{Integration Time, and } T_d = \text{All other delays (read-out, processing, transfer)} \quad (2)$$

The LSST Guider/Mount Servo loop also includes a fixed frequency integrator running at 1KHz to increase the low frequency gain, an adjustable loop gain parameter which is optimized, depending on the frame rate and transport delays, a 20Hz ZOH at the TCS interface, and a simplified Telescope Mount model consisting of a 2Hz second order low pass filter, with damping coefficient of 0.5.

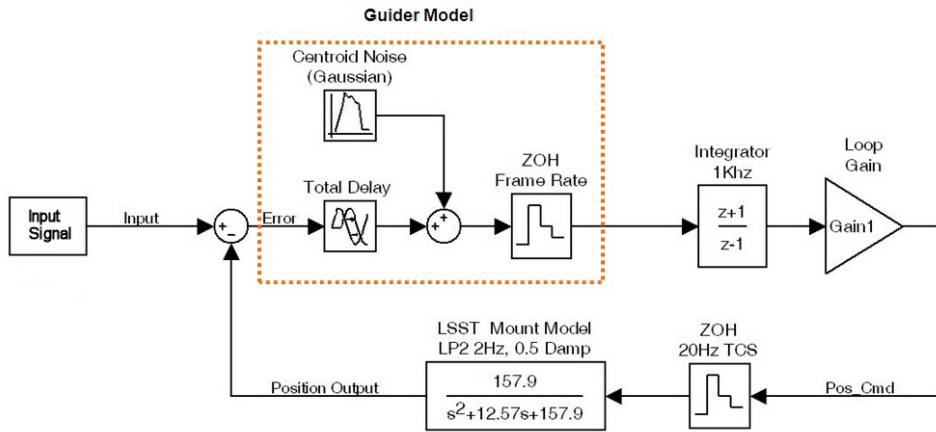


Figure 11. LSST Guider/Mount Servo Loop Model

This model is useful to understand the overall servo performance as a function of integration time and delays. A useful Servo Loop metric is the error rejection bandwidth. The Bode plot of several simulation results for multiple integration times T_{int} , with a constant $T_d=10\text{ms}$, is shown on Figure 12.

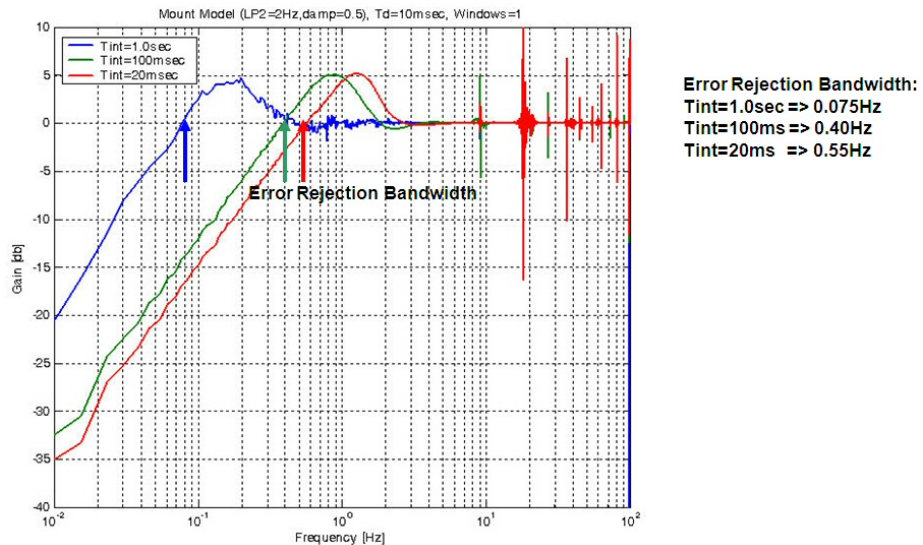


Figure 12. LSST Guider/Mount Servo Loop Error Rejection Plot

The Guider/Mount Servo Loop Model was also used to understand the effects of the centroid noise in the telescope jitter. As the centroid noise is Gaussian, it was introduced into the Servo Loop as a disturbance. Because the Guider/Mount Servo Bandwidth is smaller than the noise bandwidth, the servo acts as a low pass filter, reducing the centroid noise contribution in pointing jitter. The results of a parametric analysis (T_{int} and T_d), versus centroid noise reduction is shown in Figure 13. At the nominal 100ms integration time, a centroid error gain value of ~ 0.5 is obtained. This is the value used in the centroid noise requirements analysis in Section 2.3.

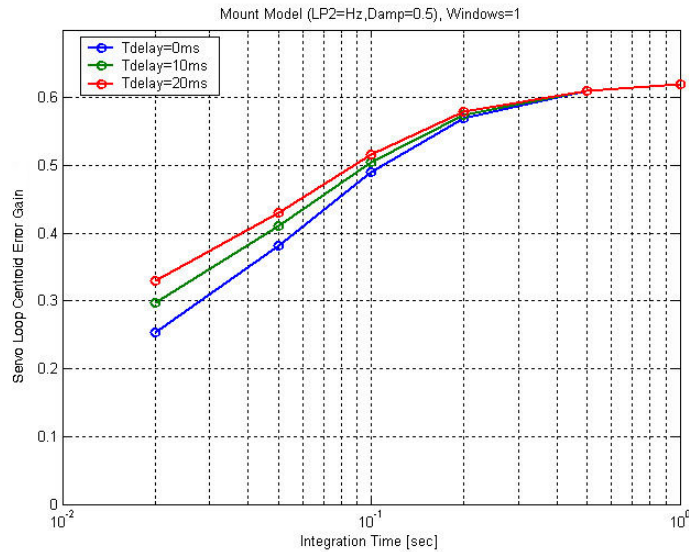


Figure 13. LSST Guider/Mount Servo Loop Centroid Error Gain

3.2 LSST Atmospheric Tilt Decorrelation Model

Due to the large field of view of LSST camera, the atmospheric turbulence signal seen at the guider groups, located at the corner rafts, will be only partially correlated. A simple geometric model (Figure 14) shows that the tilt from ground and low atmospheric layers (<136 m), will be mostly correlated, and that middle to upper atmospheric layer disturbance signal (>136 m), will be mostly decorrelated between the guider groups. A problem arises when using this signal for guiding, as the decorrelated component signal will appear as uncorrected jitter and degrade the image, for areas away from the guider sensor FOV.

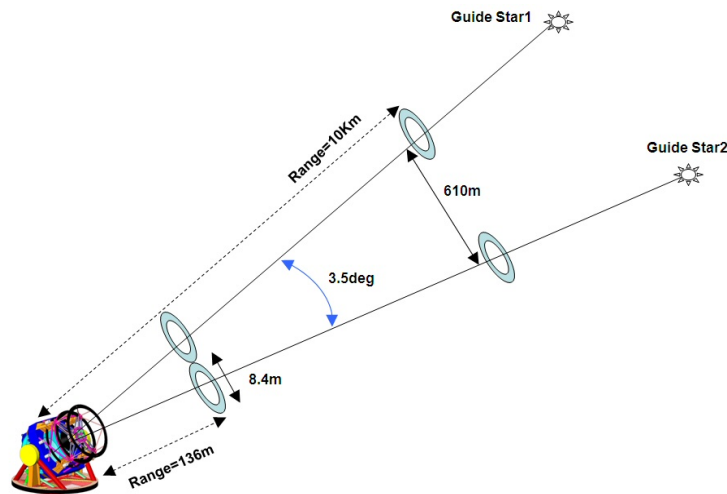


Figure 14. Atmospheric model for LSST guiding.

A 7-layer atmospheric tilt model for Cerro Pachon, considering the large central obscuration of the LSST primary mirror, was developed by Andrei Tokovinin⁸. The turbulence integrals for each altitude used on this model, are shown in Table 2.

Table 2. 7-Layer Tilt Model for Cerro Pachon, turbulence, J in units of $10^{-13} \text{m}^{1/3}$ are given.

H , km	Good	Typ.	Bad	V , m/s	Dir., deg.
0	2.2	2.7	3.3	5	0
0.5	0.2	0.4	0.7	7	0
1	0.03	0.1	0.2	7	0
2	0.02	0.1	0.4	8	315
4	0.2	0.4	0.6	18	270
8	0.15	0.2	0.3	38	270
16	0.25	0.3	0.3	8	270
J_{tot}	3.05	4.2	5.8	-	-
β''	0.62	0.74	0.85	-	-

The 7-layer atmospheric tilt model allows calculating the Power Spectral Density (PSD) for the tilt component associated with each layer, as shown in Figures 15a and Figure 15b, for an Air Mass=1, and outer scale $L_0=25\text{m}$. The model was also used to calculate the Cross-Spectral Density between 2 sensors separated by a known angle. When a separation of 3.5 degrees was used, the Cross-Spectral Density shows that there is no correlation at the higher layers, and a good correlation at the ground layer, as expected. Based on the decorrelation of the upper layers, a simpler model was built combining all the uncorrelated upper layers into one tilt component, and the lower layer kept as the correlated tilt component. Separating these 2 signals from each other was useful in understanding the effects of guider tracking, with a partially correlated signal on a large field of view system such as LSST.

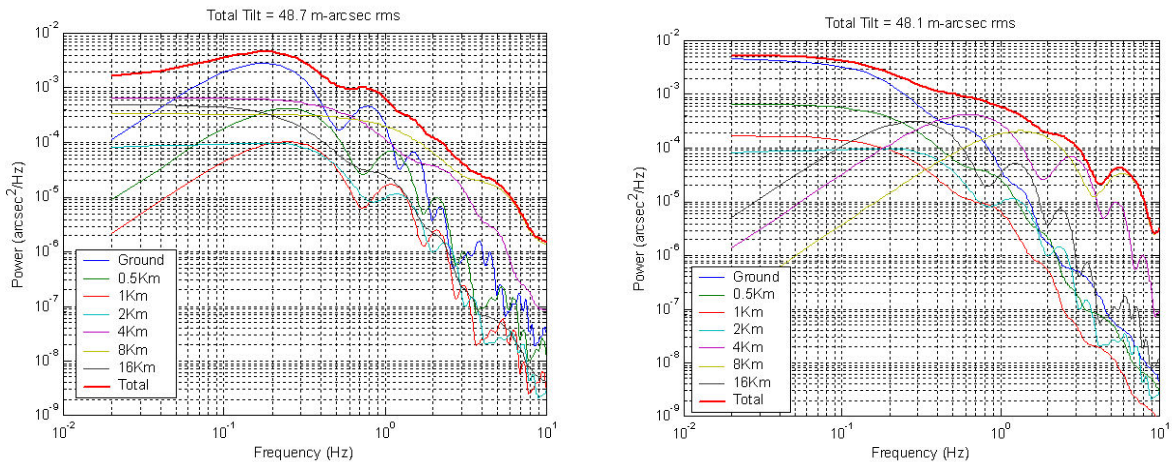


Figure 15a (left). LSST Atmospheric Tilt Power Spectral Density, N-S direction, Typical Seeing, AM=1, $L_0=25\text{m}$
 Figure 15b (right). LSST Atmospheric Tilt Power Spectral Density, E-W direction, Typical Seeing, AM=1, $L_0=25\text{m}$

The total tilt from all layers for a single guider for the nominal case is shown in Figure 15 and summarized in Table 3. The upper layer tilt jitter is higher than the lower layers. This uncorrelated jitter can be reduced by combining the four guider group signals.

Table 3. LSST Single Guider Tilt jitter, AM=1.0, L₀=25 mts.

Layer	Tilt Jitter
Lower Layer N-S	0.03127 arc-sec rms
All Upper Layer N-S	0.03843 arc-sec rms
Total N-S	0.04891 arc-sec rms
Lower Layer E-W	0.03005 arc-sec rms
All Upper Layer E-W	0.03852 arc-sec rms
Total E-W	0.04919 arc-sec rms

3.3 LSST Atmospheric Correction Simulation

With the 7-layer atmospheric model, and a Guider/Mount servo loop described in 3.2, the contribution of atmospheric decorrelation in the telescope tracking jitter was analyzed. For this, the average Power Spectral Density (PSD) values for the ground and upper layers shown in Figure 15a, and Figure 15b, were combined to produce a ground and upper layer average of both N-S, and E-W components. The resulting PSD's were used to synthesize time domain sequences by convolving the tilt PSD's with Gaussian noise, and then performing an Inverse Fourier Transform to obtain time domain sequence. These synthetic tilt waveforms were used as input to the models described in Figure 11, where the ground layer is fed as input, and the averaged upper layer is fed as a noise disturbance. The resulting tilt PSD is shown in Figure 16, where the values were obtained for the nominal seeing case, an Air Mass=1, and outer scale of L₀=25m. The pointing error obtained with this simulation indicates that the gain in tracking jitter achieved by correcting the lower layer tilt is lost by the increase in tracking jitter due to the decorrelated upper layer.

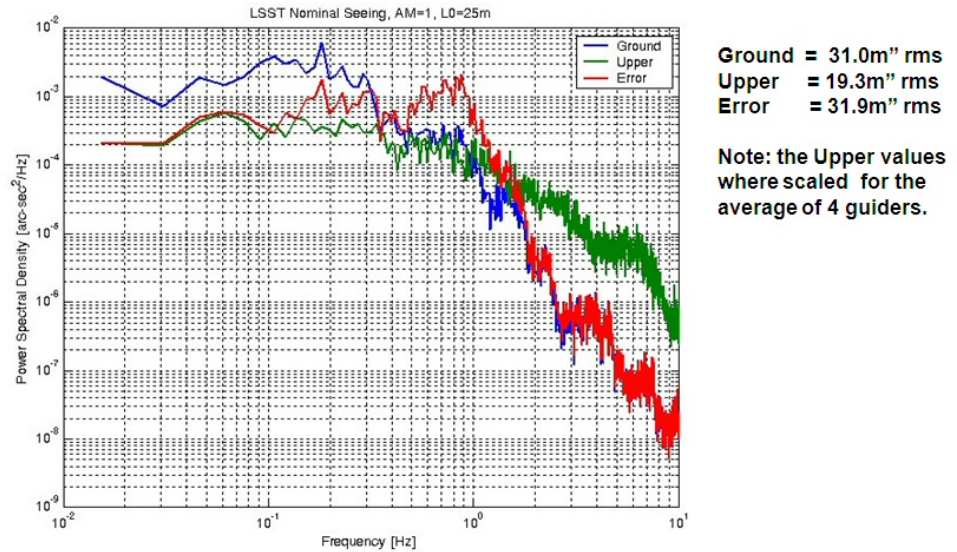


Figure 16. LSST Guider/Mount Servo Loop Centroid Error Gain

4. CONCLUSIONS

We have developed a complete model of the Guider/Mount Servo Loop, including a worst case scenario where all the variables were taken to their extreme cases. These results indicate that the centroid jitter requirements can be met under all conditions, with adequate margin. Future refinements to this work include adding the population and spectra of known low magnitude guide stars, which should improve the flux in the Y band filter bands.

The simulation showing the effects of atmospheric decorrelation needs to be further investigated, as atmospheric decorrelation introduces a jitter source, which depends on the height and intensity of the atmospheric turbulence, since in some cases closing the guider loop can introduce a small amount of unwanted tracking jitter. Real time turbulence profiles versus altitude will be needed to predict the improvement or degradation in tracking jitter due to atmospheric decorrelation. Another method is to perform cross-correlation of the signals between the different guider groups to obtain an estimate of the decorrelated atmospheric tilt power.

ACKNOWLEDGEMENT

LSST is a public-private partnership. Funding for design and development activity comes from the National Science Foundation, private donations, grants to universities, and in-kind support at Department of Energy laboratories and other LSSTC Institutional Members. This work is supported by in part the National Science Foundation under Scientific Program Order No. 9 (AST-0551161) and Scientific Program Order No. 1 (AST-0244680) through Cooperative Agreement AST-0132798. Portions of this work are supported by the Department of Energy under contract DE-AC02-76SF00515 with the Stanford Linear Accelerator Center and contract DE-AC52-07NA27344 with Lawrence Livermore National Laboratory. LLNL-PROC-436311.

REFERENCES

- [1] R. J. Dorn, et al, "Evaluation of the Teledyne SIDECAR ASIC at cryogenic temperature using a visible hybrid H2RG focal plane array in 32 channel readout mode", Proc. of SPIE Vol. 7021, 70210Q, (2008)
- [2] R. J. Dorn, et al, "A CMOS visible silicon imager hybridized to a Rockwell 2RG multiplexer as a new detector for ground based astronomy", Proc. SPIE, Vol. 6276, 627607H (2006)
- [3] LSST Operations Cadence Simulator, <http://www.noao.edu/lst/opsim/>
- [4] Vega Spectrum: ftp://ftp.stsci.edu/cdbs/current_calspec/alpha_lyr_stis_005.ascii
- [5] C. W. Allen, "Astrophysical Quantities", University of London, Athlone Press; 3rd edition (1973)
- [6] Sandrine Thomas, "Optimized centroid computing in a Shack-Hartmann sensor", Proc. SPIE 5490, 1238 (2004)
- [7] Zeljko Ivezic, Lynne Jones, and Robert Lupton, "The LSST Photon Rates and SNR Calculations, v1.2", LSST DocuShare, LSE-40.
- [8] Andrei Tokovinin, "Tilt Covariance for LSST", Version 2.1, Oct 6, 2006, LSST DocuShare, Document-2582